JOURNAL OF BACTERIOLOGY, Nov. 1994, p. 6470–6478
0021-9193/94/$04.00+0

Vol. 176, No. 21

Escherichia coli Possesses Two Homologous Anaerobic C_4-Dicarboxylate Membrane Transporters (DcuA and DcuB) Distinct from the Aerobic Dicarboxylate Transport System (Dct)

STEPHAN SIX,[1]* SIMON C. ANDREWS,[2] GOTTFRIED UNDEN,[1] AND JOHN R. GUEST[2]

Institut für Mikrobiologie und Weinforschung, Johannes Gutenberg-Universität, 55099 Mainz, Germany,[1] and The Krebs Institute, Department of Molecular Biology and Biotechnology, University of Sheffield, Sheffield S10 2UH, United Kingdom[2]

Received 28 June 1994/Accepted 25 August 1994

The nucleotide sequences of two *Escherichia coli* genes, *dcuA* and *dcuB* (formerly designated *genA* and *genF*), have been shown to encode highly homologous products, M_r 45,751 and 47,935 (434 and 446 amino acid residues) with 36% sequence identity (63% similarity). These proteins have a high proportion (~61%) of hydrophobic residues and are probably members of a new group of integral inner membrane proteins. The locations of the *dcu* genes, one upstream of the aspartase gene (*dcuA-aspA*) and the other downstream of the anaerobic fumarase gene (*fumB-dcuB*), suggested that they may function in the anaerobic transport of C_4-dicarboxylic acids. Growth tests and transport studies with mutants containing insertionally inactivated chromosomal *dcuA* and *dcuB* genes show that their products perform analogous and mutually complementary roles as anaerobic dicarboxylate carriers. The anaerobic dicarboxylate transport systems (Dcu) are genetically and functionally distinct from the aerobic system (Dct).

Escherichia coli can utilize C_4-dicarboxylic acids to support both aerobic and anaerobic respiratory growth. Under aerobic conditions, dicarboxylate uptake is mediated by the binding protein-dependent Dct system (13). The Dct membrane components are thought to be encoded by the *dctA* and *dctB* genes and the periplasmic binding protein is thought to be encoded by the *cbt* gene, but neither the genes nor their products have been thoroughly characterized. In contrast, when *E. coli* is grown anaerobically with fumarate as the electron acceptor, C_4-dicarboxylates are taken up by a specific anaerobic transport system, the Dcu system (5, 6). The anaerobic transport system has the characteristics of a secondary carrier and catalyzes homologous and heterologous exchanges of dicarboxylates, whereas the aerobic system operates only in the unidirectional (uptake) mode. The Dcu system is reversibly inhibited by oxidizing agents. Its anaerobic expression appears to be controlled by the anaerobic transcriptional activator (FNR), and it is repressed by nitrate (5, 6). The Dcu system functions as an electroneutral fumarate-succinate (precursor-product) exchanger during fumarate respiration, a key mechanism of anaerobic energy conservation.

Earlier studies on the anaerobically inducible aspartase and fumarase genes (*aspA* and *fumB*) revealed two genes, *dcuA* and *dcuB* (formerly designated *genA* and *genF*), located immediately downstream of the aspartase gene at 94.0 min (*aspA-dcuA*) (23, 27) and directly upstream of the anaerobic fumarase gene at 93.5 min (*dcuB-fumB*) (2). The two genes were only partially sequenced, but in view of their locations and hydrophobic products, they were predicted to encode homologous integral membrane proteins performing analogous functions in the anaerobic transport of aspartate and fumarate (2). In order to explore this possibility, the nucleotide sequences of the *dcuA* and *dcuB* genes were completed and the effects of replacing the chromosomal genes with insertionally inactivated derivatives on both bacterial growth and C_4-dicarboxylic acid transport were investigated. The results strongly indicate that the *dcuA* and *dcuB* products have analogous and mutually complementary transport functions in anaerobic C_4-dicarboxylate transport.

* Corresponding author. Mailing address: Institut für Mikrobiologie und Weinforschung, Johannes Gutenberg-Universität, 55099 Mainz, Germany. Phone: 49 6131 393551. Fax: 49 6131 392695.

MATERIALS AND METHODS

Bacterial stains, plasmids, bacteriophages, and growth conditions. The strains of *E. coli* K-12 used were JM101 (*thi supE ΔproAB-lac*/F' *traD36 proA*$^+$*B*$^+$ *lacI*^{q}*ZΔM15*), host for M13, pBR325, pBR322, ColE1, and pUC derivatives (16); JC7623 (*recBC sbcBC*) for genomic replacement studies (18); and AN387, the wild-type parental strain, for studying the effects of *dcuA* and *dcuB* inactivation. The source plasmids used for completing the *dcu* sequences and insertionally inactivating the *dcu* genes were a pBR325 derivative, pGS71 (9); a pBR322 derivative, pGS73 (9); and a ColE1 derivative, pGS79 (8) (see Fig. 1). M13mp18 and M13mp19 were used for subcloning and preparing templates for DNA sequencing. P1 transduction was done according to the method of Miller (17). Bacteriophage and plasmid DNA were isolated and manipulated according to the method of Sambrook et al. (20). Bacteria were routinely grown at 37°C in LB medium (17) for DNA manipulation and genetic studies and in M9 minimal medium (17) for growth tests and transport measurements. The minimal medium was supplemented with 1 mM $MgSO_4$–0.1% acid-hydrolyzed casein–50 mg of tryptophan per liter and either 0.4% glucose or 0.4% glycerol plus 50 mM fumarate, malate, or aspartate under anaerobic conditions or 50 mM succinate under aerobic conditions. For anaerobic growth, bacteria were grown in degassed media in rubber-stoppered infusion bottles under N_2.

DNA sequence analysis. The 1-kb *Bam*HI-*Hin*dIII fragment of pGS79 (8) and the 0.5-kb *Bcl*I fragment of pGS71 (9), containing the unsequenced regions of the respective *dcuB*

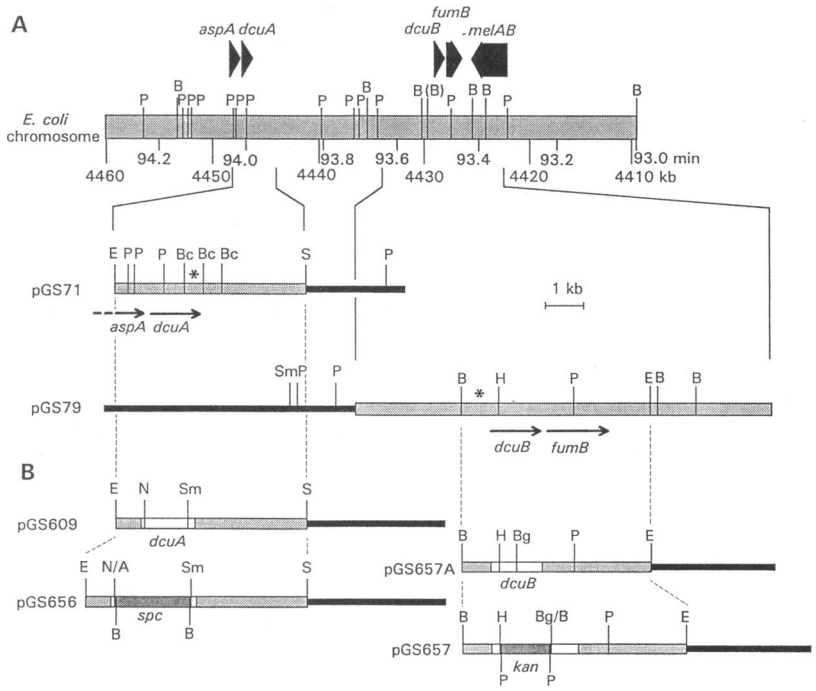

FIG. 1. Relative positions of the *dcuA* and *dcuB* genes in the *E. coli* chromosome and source plasmids pGS71 and pGS79. (A) Locations and transcriptional polarities of the *aspA*, *dcu*, and *fumB* genes are shown with scales to identify the positions (in minutes) in the *E. coli* linkage map (1) and the nucleotide coordinates (in kilobases) in the physical map (11). Lightly shaded bars represent chromosomal DNA, solid bars represent plasmid DNA, and asterisks denote fragments used for nucleotide sequence analysis. (B) Plasmids containing insertionally inactivated *dcu* genes and their immediate precursors are shown with relevant restriction sites only. The *dcu* genes (open bars) and antibiotic resistance cassettes (darkly shaded bars) are indicated. Restriction sites are as follows: A, *Acc*I; B, *Bam*HI; Bc, *Bcl*I; Bg, *Bgl*II; E, *Eco*RI; H, *Hin*dIII; N, *Nar*I; P, *Pst*I; S, *Sal*I; Sm, *Sma*I; N/A and Bg/B, hybrid restriction sites no longer recognized by corresponding restriction enzymes; (B), a *Bam*HI site in the physical map of Kohara et al. (11) which is absent from the corresponding region of pGS79.

(*genF*) and *dcuA* (*genA*) genes (see Fig. 1), were subcloned in M13mp18 and M13mp19. Both DNA strands were sequenced from single-stranded M13 templates by using Sequenase (22) with universal and specific oligonucleotide primers. Nucleotide sequences were compiled and analyzed with computer programs (21), and sequence databases were searched via the SERC Seqnet Facility at the Daresbury Laboratory, Daresbury, United Kingdom.

Gene replacement, chromosomal DNA isolation, and Southern blotting. Genomic replacement was achieved by the method of Oden et al. (18). For this purpose two plasmids, pGS656 (*dcuA*::Spc^r) and pGS657 (*dcuB*::Kan^r), containing disrupted *dcuA* and *dcuB* genes were constructed (see Fig. 1). The former involved subcloning the 2-kb *Bam*HI spectinomycin resistance cassette of pUX-Ω (19) into pUC118 (24) to generate pGS606 and provide the Spc^r cassette with flanking *Sma*I and *Acc*I sites. The 5.0-kb *Eco*RI-*Sal*I *dcuA* fragment of pGS71 was cloned into pBR322 (3) to generate pGS609 (see Fig. 1), and the 1.2-kb *Nar*I-*Sma*I segment, containing most of the *dcuA* gene, was then replaced by the 2.0-kb *Acc*I-*Sma*I Spc^r cassette from pGS606 to give pGS656. The construction of pGS657 first involved cloning the *Pst*I-treated 1.3-kb kanamycin resistance GenBlock fragment (Pharmacia) into the pUC118 multicloning site to produce pGS607 and provide flanking *Hin*dIII and *Bam*HI sites for the Kan^r cassette. The 4.7-kb *Eco*RI-*Bam*HI *dcuB-fumB* fragment of pGS79 was then cloned into pGS608 (a pUC118 derivative lacking the *Hin*dIII site) to give pGS657A (see Fig. 1), and in the final step, the 0.4-kb *Hin*dIII-*Bgl*II internal *dcuB* fragment was replaced by the 1.3-kb *Hin*dIII-*Bam*HI Kan^r cassette from pGS607 to generate pGS657.

Southern blotting (20) was performed with *Pst*I or *Bam*HI restriction digests of *E. coli* chromosomal DNA isolated according to the procedure of Marmur (15). Hybridization probes were prepared by random-primed DNA polymerase I (Klenow)-dependent incorporation of digoxigenin-11-dUTP into double-stranded restriction fragments. The following probes were used: a 2-kb *Bam*HI Spc^r fragment from pGS606, a 1.3-kb *Pst*I Kan^r fragment from pGS607, a 5.0-kb *Eco*RI-*Sal*I *dcuA* fragment from pGS609, and a 4.7-kb *Bam*HI-*Eco*RI *dcuB* fragment from pGS657A (see Fig. 1). The prehybridization, hybridization, and washing conditions were those described by Sambrook et al. (20), and immunodetection was performed according to the manufacturer's instructions (Boehringer Mannheim). Molecular weight markers were prepared by labeling *Hin*dIII and *Hin*dIII-plus-*Eco*RI digests of λ DNA with digoxigenin-11-dUTP by T4 DNA polymerase-dependent replacement synthesis (20).

Transport assays. Transport activity was measured by determining the exchange of intracellular and extracellular C_4-dicarboxylates. Unless stated otherwise, this involved using the silicone oil centrifugation method to measure the uptake of [^{14}C]fumarate into succinate-loaded bacteria (5, 6). The internal concentration of succinate after the loading procedure was at least 30 (JRG2814) to 75 times (AN387) higher than the external concentration of [^{14}C]fumarate used. Buffer A contained 20 mM glucose and 2 mM dithiothreitol in the anaerobic transport assays. The standard deviations for exchange activities at a 20 μM external concentration of [^{14}C]fumarate were 7.3 ± 1.9 (AN387), 6.7 ± 3.1 (JRG2813), 7.9 ± 1.6 (JRG2821), and 2.0 ± 0.4 μmol/min/g of dry cells (JRG2814). For measuring exchange activities for various C_4-dicarboxy-

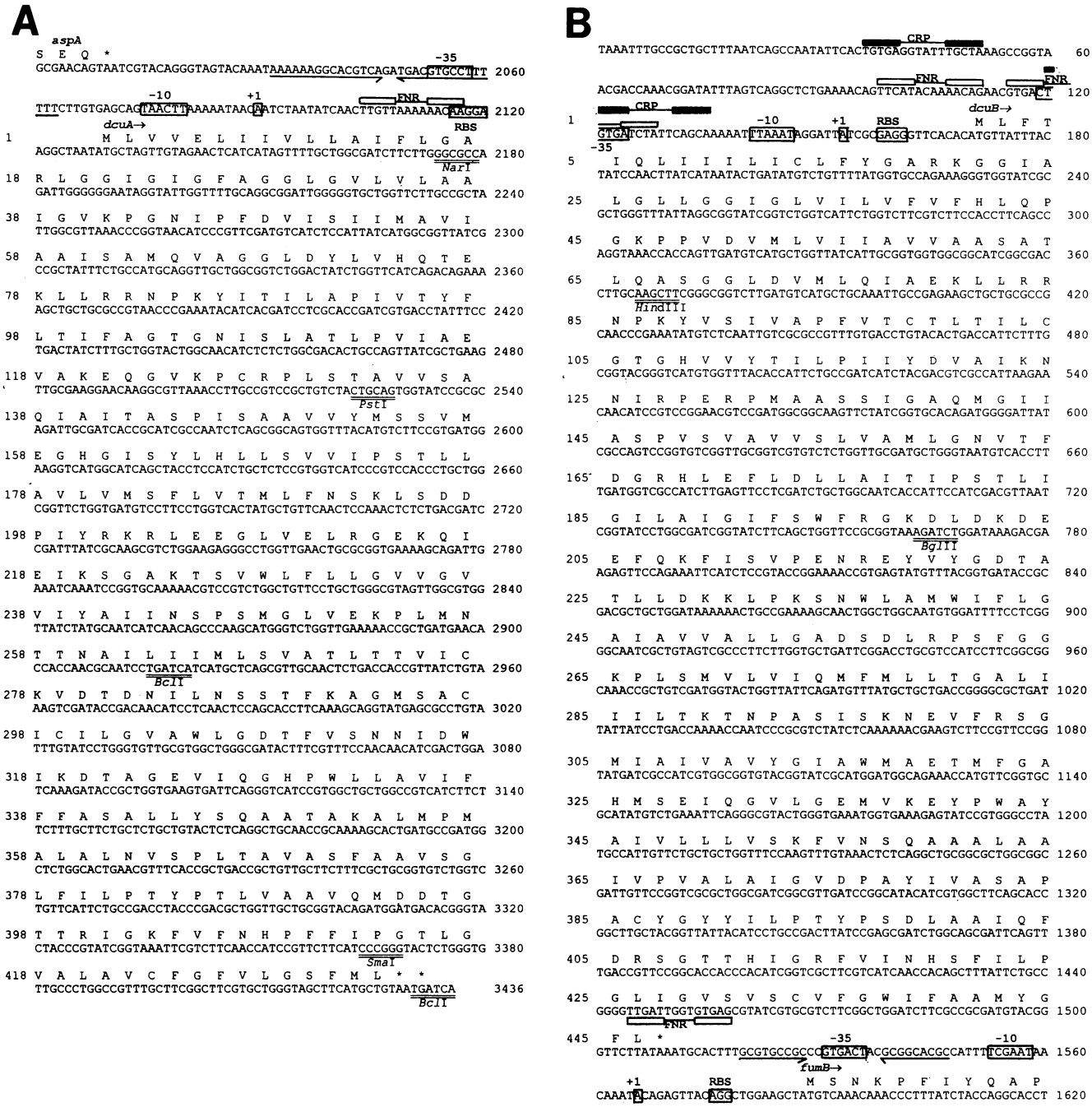

FIG. 2. Complete nucleotide sequences of the *dcuA* and *dcuB* genes and primary structures of their products, DcuA and DcuB. The nucleotide coordinates are extended from those used previously for the *aspA-dcuA* region (27) but redefined for the *dcuB-fumB* region. Relevant restriction sites are double underlined; potential ribosome-binding sites (RBS) and the −35, −10, and +1 sites of putative promoters are indicated by boxes; two potential *rho*-independent transcriptional terminators are indicated by converging arrows; and the positions of potential FNR- and CRP-binding sites are indicated by open and solid bars, respectively.

lates (as shown in Fig. 8), anaerobic cell suspensions (A_{578} = 3 to 4) were preloaded with [2,3-^{14}C]succinate (100 μM for 15 min), intracellular radioactivity was estimated, and unlabeled C_4-dicarboxylate (10 mM final concentration) was added at time zero. Residual [^{14}C]succinate was then determined after 20 s by the silicone oil centrifugation method. Specific exchange activities were calculated from the decreases in intracellular radioactivity (6). The effects of competitive inhibition by other C_4-dicarboxylates were determined as follows: succinate-loaded cell suspensions (A_{578} = 3 to 4) were incubated with 50 μM [2,3-^{14}C]succinate in the presence or absence of 500 μM unlabeled dicarboxylate. The uptake of the labeled substrate is presented as a percentage of the uptake observed in the absence of unlabeled substrate. The uptake of [^{14}C]fumarate into aerobically grown bacteria was performed as described for the anaerobic exchange of fumarate, but without

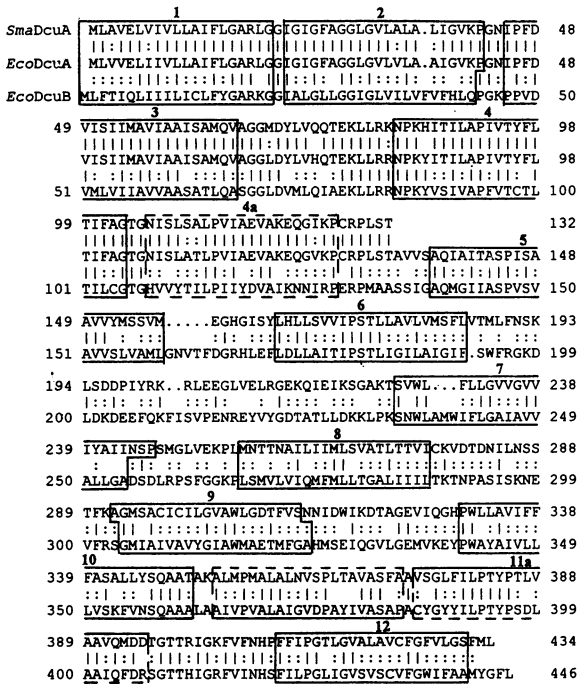

FIG. 3. Alignment of the complete DcuA and DcuB amino acid sequences of *E. coli* K-12 and the incomplete DcuA sequence of *S. marcescens*. The sequences were aligned with the GAP computer program. Conserved residues (vertical bars), conservatively substituted residues (colons), and insertions or deletions (periods) are indicated. The twelve strongly predicted membrane-spanning helices are boxed, and the two tentatively predicted spanners are outlined by broken lines.

preloading the bacteria with succinate and using buffer A without degassing and dithiothreitol.

Nucleotide sequence accession numbers. The *dcuA* and *dcuB* nucleotide sequences have been submitted to the EMBL database under accession numbers X79887 and X79886, respectively.

RESULTS

Nucleotide sequences of the *dcuA* and *dcuB* genes. The possibility that the *dcuA* and *dcuB* genes (formerly *genA* and *genF*) might encode analogous integral membrane proteins involved in the transport of aspartate and fumarate (2) was based on their locations immediately upstream and downstream of the *aspA* and *fumB* genes and on the hydrophobicities and sequence similarities of the partial amino acid sequences of the predicted gene products. In order to explore this possibility, the complete nucleotide sequences of the two *dcu* genes were defined and the physiological consequences of their inactivation were investigated.

Alignments of the incomplete DcuA and DcuB amino acid sequences indicated that they derive from homologous proteins lacking approximately 23 and 64 residues at their respective C- and N-terminal ends. Appropriate segments were accordingly isolated from the *dcuA-aspA* and *fumB-dcuB* plasmids for completing the *dcu* sequences (Fig. 1). For *dcuA*, this involved defining the sequence of the entire 521-bp *Bcl*I fragment of pGS71 adjacent to the previously sequenced 2,921-bp *aspA-dcuA'* region (27). Continuity was established by reference to an analogous but overlapping partial sequence from *E. coli* W (23). For *dcuB*, the previously sequenced 3,162-bp *dcuB'-fumB* fragment (2) was extended by 372 bp from the *Hin*dIII site in the 1-kb *Bam*HI-*Hin*dIII fragment of pGS79 (Fig. 1). The complete sequences of the *dcuA* and *dcuB* segments of the 3,430-bp *aspA-dcuA* and 3,588-bp *dcuB-fumB* sequences are shown in Fig. 2, and translations of the two coding regions, identified by their codon preferences, are also included.

The *dcuA*, *dcuB*, and *fumB* genes are all associated with well-predicted σ^{70} promoter sequences (Fig. 2), and the *aspA-dcuA* and *dcuB-fumB* intergenic regions contain potential *rho*-independent terminator sequences. These observations suggested that each member of the two gene pairs, *aspA-dcuA* and *dcuB-fumB*, could represent independent transcription units, although the possibility that each pair might be coregulated or even cotranscribed from an upstream promoter was not excluded.

The promoter regions of all four genes were searched for potential FNR- and cyclic AMP receptor protein (CRP)-binding sites by using score matrices derived from 22 FNR sites and 25 CRP sites. The *aspA* promoter region has overlapping FNR- and CRP-binding sites centered at −36.5 (coordinates 379 and 380) and −97.5 (coordinates 318 and 319) relative to potential promoter C (27) in addition to two potential FNR sites centered further upstream (coordinates 186 and 187 and coordinates 197 and 198) (27). The *dcuB* promoter region, likewise, has well-placed potential FNR and CRP sites (Fig. 2B). In contrast, the *aspA-dcuA* and *dcuB-fumB* intergenic regions contain only one potential FNR site, poorly placed for a role in FNR-mediated activation of the putative *fumB* promoter, and no predicted CRP sites (Fig. 2). These observations tend to support the view that global regulation may be imposed at the upstream *aspA* and *dcuB* promoters during cotranscription of the two gene pairs.

The *dcuA* and *dcuB* coding regions are each preceded by well-placed ribosome-binding sites (Fig. 2), and the translational initiation sites were predicted by Perceptron analysis (21). The *aspA* and *dcuA* codon usages correspond to those of strongly expressed genes (69.3 and 66.5% use of optimal energy codons, respectively) (7), whereas those of *dcuB* and *fumB* suggest that they are moderately expressed (56.4 and 56.6% use of optimal codons). This indicates that the *aspA* and *dcuA* products may be more abundant than those of *dcuB* and *fumB* when the genes are maximally induced.

There are five differences between the nucleotide sequence of the *dcuA* gene of *E. coli* K-12 (Fig. 2A) and the partial sequence of the corresponding *E. coli* W gene (23): positions 3193 and 3194 in *E. coli* K-12 are GC rather than CG; position 3220 is A rather than T; and positions 3222 and 3229 each represent single C insertions. The *dcuA* coding region of *E. coli* W was originally reported to terminate at a TGA codon, positions 3225 to 3227, and the present results support an earlier prediction that the insertion of 2 bp near this stop codon would extend the open reading frame by a further 46 codons and continue the similarity with *dcuB* to the end of the sequenced region (2). The three nucleotide substitutions generate a silent mutation in the S-364 codon and two relatively conservative replacements (M-335→I and P-336→A) in the DcuA of *E. coli* W, which could be genuine strain differences.

The primary structures deduced for the DcuA and DcuB proteins are aligned in Fig. 3. They exhibit 36% sequence identity (63% similarity), and the proteins are of similar size and composition, M_r 45,751 (434 residues) and 47,935 (446 residues), respectively. Both proteins have a high proportion (~61%) of hydrophobic amino acids, and they appear to lack N-terminal signal sequences, indicating that they are probably

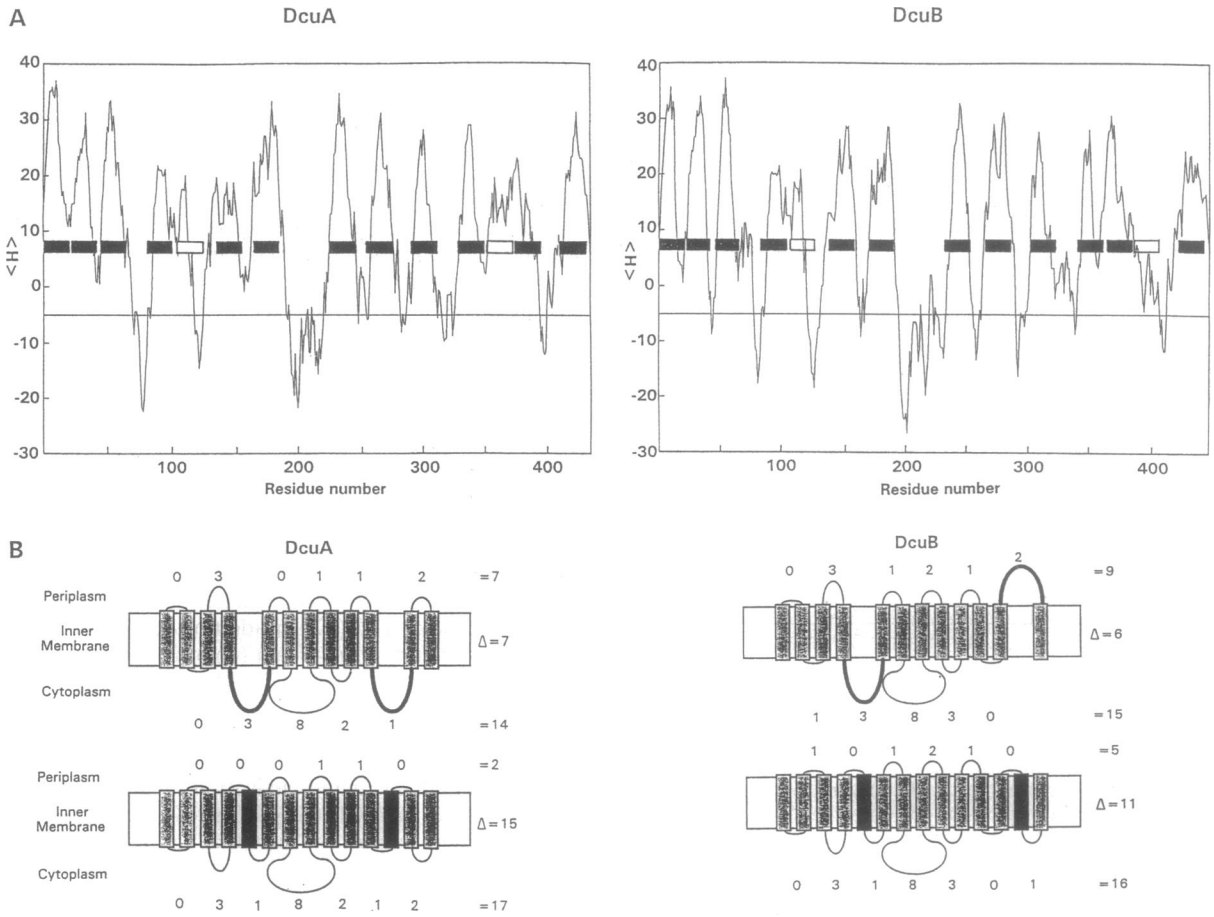

FIG. 4. (A) Hydropathy plots of the DcuA and DcuB proteins. Consecutive hydropathy averages (<H>) for 11-residue spans calculated according to the method of Kyte and Doolittle (12) are plotted versus amino acid residue number. Strongly and tentatively predicted transmembrane segments are indicated by solid and open bars, respectively. (B) Alternative membrane topology predictions for the DcuA and DcuB proteins. Tentatively predicted transmembrane segments (black bars) are shown in the lower diagrams, and their sources (thick lines) are shown in the upper diagrams. The combined arginine and lysine content of each polar segment and the overall charge biases (Δ) are indicated.

integral inner membrane proteins. This conclusion was further supported by SOAP and Helixmem analyses (4, 10), which predict that there are twelve membrane-spanning helices in each protein (Fig. 3 and 4). Since many bacterial secondary carriers contain twelve transmembrane helices (14), the prediction is consistent with the proposal that DcuA and DcuB are secondary carriers. Sequence comparisons with current databases revealed a 92% sequence identity between DcuA and a partial sequence of the DcuA homolog of *Serratia marcescens* (*Sm*DcuA; PIR protein sequence database accession number PS0397): the partial sequence is included in the Fig. 3 alignment. No significant similarity was detected with any other proteins, including membrane transporters, suggesting that DcuA and DcuB represent a new and independent group of bacterial membrane proteins.

The orientations of integral membrane proteins within the membrane can be predicted by applying the positive-inside rule (25). The topologies predicted for DcuA and DcuB are shown in Fig. 4B together with the corresponding charge biases. The hydropathy profiles (Fig. 4A) indicated that these proteins might contain two membrane-spanning segments in addition to the twelve predicted by SOAP and Helixmem analyses (Fig. 3).

Inactivation of the chromosomal *dcuA* and *dcuB* genes. The plasmid-encoded *dcu* genes were inactivated by replacing segments of their coding regions with antibiotic resistance cassettes of differing specificity to facilitate the construction of double mutants after chromosomal gene replacement. The *dcuA* gene was inactivated by replacing the internal 1.2-kb *Nar*I-*Sma*I fragment of pGS609 with a Spc^r cassette to generate pGS656, and the *dcuB* gene was likewise inactivated by replacing the internal 0.4-kb *Hin*dIII-*Bgl*II fragment of pGS657A with a Kan^r cassette to generate pGS657 (Fig. 1). The chromosomal *dcu* genes were then replaced by their disrupted derivative genes by homologous recombination in separate transformations of *E. coli* JC7623 (*recBC sbcBC*) with covalently closed-circular forms of pGS656 and pGS657 (18). Km^r and Sp^r transformants were selected and screened for those with Ap^s phenotypes consistent with the chromosomal gene replacement and loss of plasmids. Strains with the desired phenotypes served as donors for transferring the disrupted genes to a wild-type host (AN387) by single and sequential P1 transduction crosses to produce representative single and double mutants, JRG2821 (*dcuA*::Spc^r), JRG2813 (*dcuB*::Kan^r), and JRG2814 (*dcuA*::Spc^r *dcuB*::Kan^r). Each of the JC7623 and AN387 derivatives was tested for disruption of the corresponding parental gene and acquisition of the resistance cassette by Southern blot analysis. Representative hybridiza-

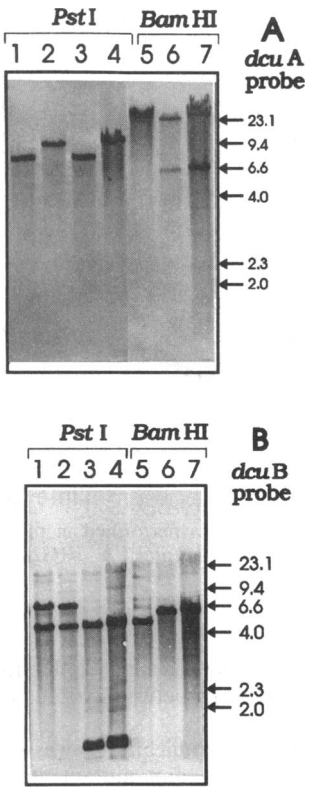

FIG. 5. Hybridization of DNA fragments from AN387 (*dcu*$^+$) and derivatives (*dcuA*::Spc^r and *dcuB*::Kan^r) with probes containing the *dcuA* (A) and *dcuB* (B) genes. DNA samples digested with *Pst*I (lanes 1 to 4) or *Bam*HI (lanes 5 to 7) were from AN387 (*dcu*$^+$) (lanes 1 and 5), JRG2821 (*dcuA*::Spc^r) (lanes 2 and 6 [in panel A only]), JRG2813 (*dcuB*::Kan^r) (lanes 3 and 6 [in panel B only]), and JRG2814 (*dcuA*::Spc^r *dcuB*::Kan^r) (lanes 4 and 7). The positions of size standards (in kilobases) are indicated by arrows. In panel A, the fragments (genotypes) hybridizing with the *dcuA*$^+$ probe and their sizes (in kilobases) were as follows [observed (predicted)]: *Pst*I (*dcuA*$^+$), 7.1 (6.6, 0.8, and 0.2); *Pst*I (*dcuA*::Spc^r), 8.7 (8.3 and 0.2); *Bam*HI (*dcuA*$^+$), >20 (18.3); *Bam*HI (*dcuA*::Spc^r), >20 and 6.4 (10.8 and 6.4). In panel B, the fragments (genotypes) hybridizing with the *dcuB*$^+$ probe and their sizes (in kilobases) were as follows [observed (predicted)]: *Pst*I (*dcuB*$^+$), 7.1 and 4.5 (6.7 and 5.0); *Pst*I (*dcuB*::Kan^r), 4.7 (twice) and 1.4 (5.0, 4.9, and 1.4); *Bam*HI (*dcuB*$^+$), 4.8 (5.1); *Bam*HI (*dcuB*::Kan^r), 6.0 (6.0).

tions with *dcu* gene probes are shown in Fig. 5. The hybridization patterns matched those predicted from the physical map of the 93- to 94-min region (Fig. 1), assuming that the *Bam*HI site designated (B) is absent and that another at coordinate 4435 is also absent or located at least 5 kb further from the site at 4453. The results confirmed that the 1.2-kb *Nar*I-*Sma*I chromosomal *dcuA* fragment had been replaced by the 2.0-kb Spc^r cassette in Sp^r strains and that the 0.4-kb *Hin*dIII-*Bgl*II *dcuB* fragment had been replaced by the 1.3-kb Kan^r cassette in Km^r strains. Hybridizations with Spc^r and Kan^r probes further confirmed that resistance cassettes were inserted at the desired sites in corresponding strains (data not shown).

Growth tests. The growth phenotypes of mutants and the isogenic parental strain were compared under different conditions (Fig. 6). No significant differences were detected during aerobic growth with succinate as the carbon source or during anaerobic growth with glucose. However, during anaerobic growth with glycerol plus either fumarate, malate, or aspartate, the double mutant was severely impaired, whereas single mutants were either unaffected or less affected, depending on the C_4-dicarboxylate. Malate and aspartate are known precursors of fumarate under anaerobic conditions, and it has been suggested that their uptake is mediated by the same anaerobic dicarboxylate uptake system as that for fumarate (5). In contrast, anaerobic growth with formate and nitrate was not affected for the *dcuA dcuB* double mutant.

Dicarboxylate antiport activities in *dcuA* and *dcuB* mutants. In *E. coli* grown anaerobically with dicarboxylates such as fumarate, malate, or aspartate plus an electron donor, high activities can be measured for dicarboxylate exchange (5, 6). The activity was determined following silicone oil centrifugation as the uptake of [^{14}C]C_4-dicarboxylates (fumarate or succinate) into cells loaded with succinate (or other C_4-dicarboxylates). Loading provides the cells with an internal substrate for exchange. The apparent K_m and maximum rate of transport (V_{max}) values for the fumarate uptake activities of the mutant and parental strains were determined from Lineweaver-Burk plots (Fig. 7; Table 1). The K_m values of all strains were similar and the plots appeared to be monophasic, indicating that no more than one transport system is involved. The rates for fumarate-succinate exchange (V_{max}) were likewise similar except for the double mutant, whose rates were reduced to about 25% of the wild type (Table 1).

Substrate specificities of dicarboxylate exchange in *dcuA* and *dcuB* mutants. Wild-type *E. coli* catalyzes homologous and heterologous exchanges of fumarate, succinate, malate, and aspartate as substrates (5, 6). Therefore, the antiport activities of the *dcu* mutants and wild-type strain with various C_4-dicarboxylates were measured to determine whether the mutant strains have the same substrate specificities as the wild type. Bacterial cell suspensions were loaded with [^{14}C]succinate, and the export of internal [^{14}C]succinate was then initiated by the addition of various C_4-dicarboxylates in 100-fold excess (Fig. 8). Since export is coupled to uptake (6), a measurement of export provides an estimation of exchange activity. In the wild type, significantly higher efflux rates of intercellular succinate were achieved with external fumarate or malate as driving counter substrates than with external succinate or aspartate. In single mutants, the [^{14}C]succinate efflux rates with external fumarate, succinate, and aspartate were similar to those of the wild type, whereas the efflux rate with external malate was reduced to 78% of the wild-type level in the *dcuA* mutant and to about 27% in the *dcuB* mutant. Thus, in the *dcuB* mutant, malate is the least efficient antiport substrate, whereas it is the most efficient in the wild type.

In the double mutant, there is still some [^{14}C]succinate export stimulated by external C_4-dicarboxylates. However, this residual transport activity was not stimulated by external aspartate (Fig. 8). In general, it appears that the exchange reaction in single mutants is similar to that of the wild type with respect to activities and substrate spectra. The only significant reduction in affinity for an exchange substrate was for malate transport in the *dcuB* mutant. The residual transport activity in the double mutant, however, differs significantly from the wild type with respect to activities and substrate spectra.

Competitive inhibition of [^{14}C]succinate import by C_4-dicarboxylates. The competition between various C_4-dicarboxylates and [^{14}C]succinate as substrates for antiport activity was determined for different strains (Fig. 9) by measuring the uptake of [^{14}C]succinate into succinate-loaded cells. Competitive substrates were added to the medium in 10-fold excess (500 μM) over the [^{14}C]succinate substrate. In the wild type, the 10-fold excess of unlabeled succinate decreased the import (exchange) of [^{14}C]succinate by 75%. The reason for the

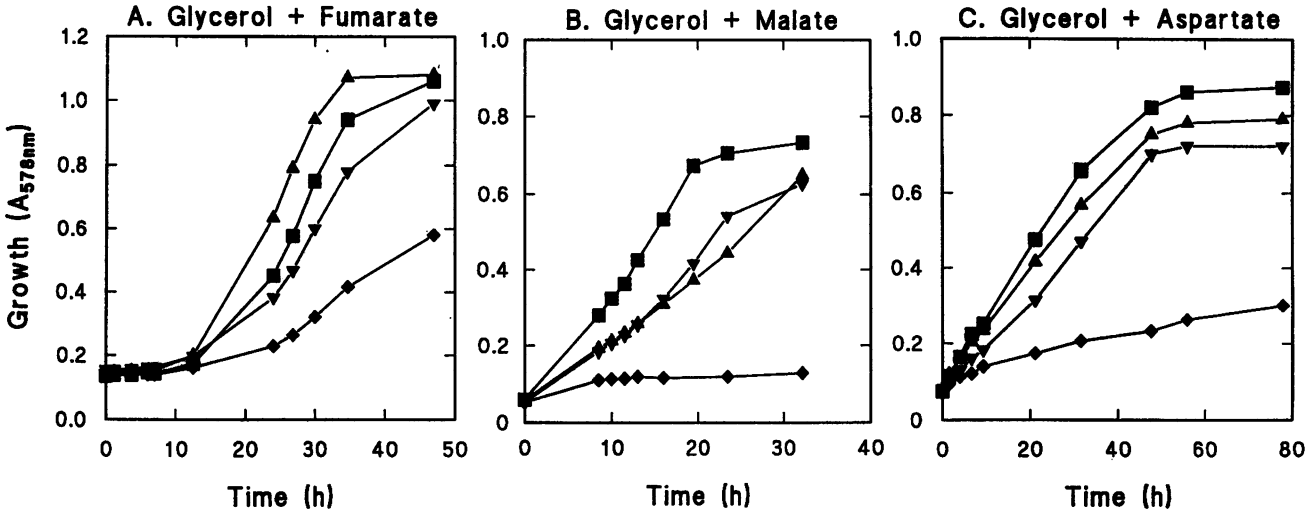

FIG. 6. Growth of *dcu* mutant and parental strains under anaerobic conditions. Growth (A_{578}) was performed in minimal media under anaerobic conditions with glycerol plus fumarate (A), malate (B), or apartate (C). ■, *E. coli* AN387 (parental); ▲, JRG2813 (*dcuB*::Spc^r); ▼, JRG2821 (*dcuA*::Spc^r); ◆, JRG2814 (*dcuA*::Spc^r *dcuB*::Kan^r).

discrepancy between the actual (75%) and expected (86%) reduction in activity is not clear. Fumarate reduced uptake activity to a similar degree as that of succinate. Malate and aspartate, however, were significantly more efficient as competitive inhibitors. Maleate, on the other hand, was only a weak competitive inhibitor of [^{14}C]succinate import. The results imply that in the wild type, C_4-dicarboxylates are accepted with the following preference: aspartate ≈ malate > fumarate > succinate >> maleate. For the *dcuA* mutant, JRG2821, very similar competitive effects were observed for the different C_4-dicarboxylates. In the *dcuB* mutant, however, the competitive effect of malate is strongly reduced. In the *dcuA dcuB* mutant, fumarate and succinate show the greatest competition followed by that of malate and then that of aspartate. In all strains, maleate had only a slight influence on succinate uptake, and the differences between strains are probably not significant.

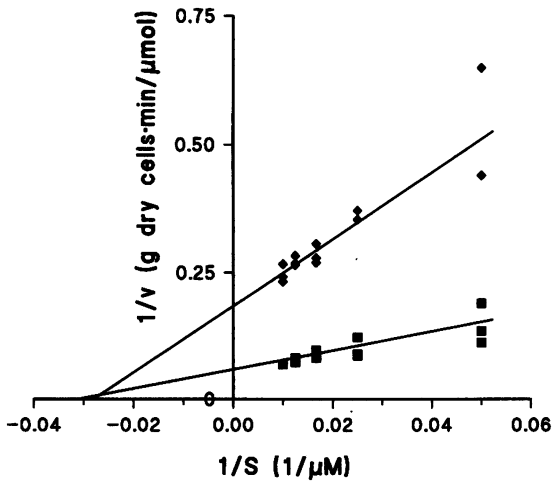

FIG. 7. Lineweaver-Burk plots for anaerobic fumarate transport. The anaerobic fumarate-succinate exchange activities of AN387 (■) and the mutant derivative JRG2814 (◆) were determined as the uptake of [^{14}C]fumarate in succinate-preloaded cells. The uptake activities (μmol/min/g of dry cells) at different fumarate concentrations (20 to 100 μM) are presented as double reciprocal plots, and K_m and V_{max} values were estimated by linear regression analysis.

Fumarate uptake in aerobically grown wild-type and *dcu* mutant strains. Wild-type and mutant strains were grown aerobically with succinate, and the K_m and V_{max} values for their [^{14}C]fumarate uptake activities were determined (Table 2). None of the mutants were significantly affected in aerobic fumarate uptake compared with that of the wild type. Therefore, inactivating the *dcuA* and *dcuB* genes, either singly or in combination, does not affect the aerobic uptake of C_4-dicarboxylates mediated by the *dctAB-cbt* system (13).

DISCUSSION

The results confirm the earlier prediction that the aspartase and anaerobic fumarase genes are adjacent to a pair of homologous genes with roles in anaerobic C_4-dicarboxylate transport. The genes have the same relative polarities, but the gene order differs: *aspA-dcuA* and *dcuB-fumB*. The *aspA* gene is subject to catabolite repression and FNR-mediated anaerobic activation, whereas the *fumB* gene is anaerobically activated by FNR but less affected by glucose-mediated repression (26). Anaerobic expression of the Dcu system also appears to be activated by the anaerobic transcriptional regulator, FNR (5). The sequences indicate that all four genes could function as independent transcriptional units. However, the distribution of potential FNR and CRP sites suggests that the two gene

TABLE 1. Apparent K_m (fumarate) and V_{max} values of [^{14}C]fumarate-succinate exchange in anaerobically grown, succinate-loaded cells[a]

Strain	K_m (μM external fumarate)	V_{max} (μmol/min/g of dry cells)
AN387 (parental)	33	18
JRG2821 (*dcuA*::Spc^r)	35	21
JRG2813 (*dcuB*::Kan^r)	30	14
JRG2814 (*dcuA*::Spc^r *dcuB*::Kan^r)	36	5

[a] Values were determined as described in the legend to Fig. 7.

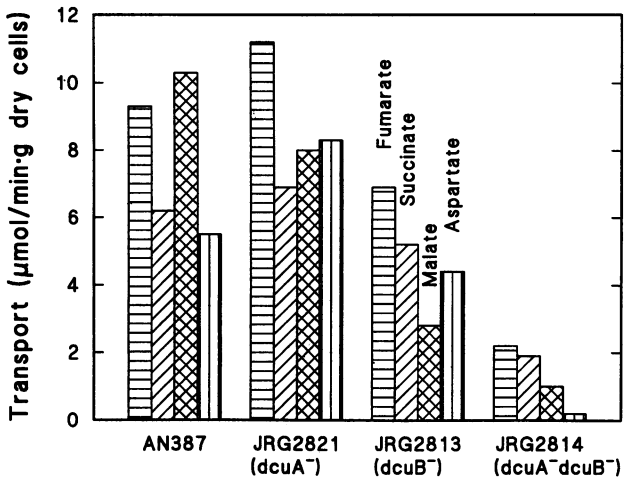

FIG. 8. Exchange rates of various C_4-dicarboxylates for wild-type *E. coli* and *dcu* mutants. Exchange activity was measured as the export of internal [^{14}C]succinate from [^{14}C]succinate-loaded cells after the addition of external substrates.

pairs are more likely to be cotranscribed from the upstream *aspA* and *dcuB* promoters.

The *dcuA* and *dcuB* genes are essential for anaerobic C_4-dicarboxylate transport. Previously, an anaerobic C_4-dicarboxylate antiport system operating during fumarate respiration was identified and characterized with respect to mechanism, energetics, and conditions of synthesis (5, 6). Under such conditions, an electroneutral exchange of dicarboxylates operates, catalyzing the import of fumarate and the concominant export of succinate. In addition to fumarate, malate and aspartate were also accepted as physiological substrates. Inactivation of the *dcuA* and *dcuB* genes decreased the anaerobic growth rate with C_4-dicarboxylates, and the antiport of these

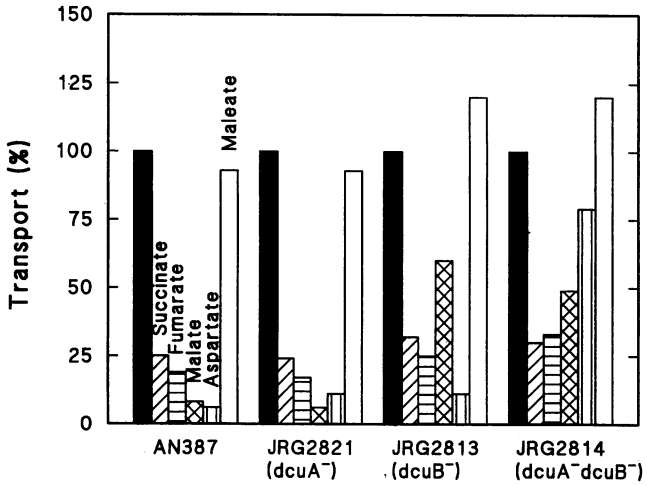

FIG. 9. Competition of [^{14}C]succinate with other C_4-dicarboxylates for transport in wild-type *E. coli* and *dcu* mutants. Exchange was measured as the uptake of [^{14}C]succinate (50 μM) into succinate-loaded bacteria in the presence of different external C_4-dicarboxylates. The exchange activity without competitive substrates was set at 100% (black bars). The absolute activities (μmol/min/g of dry cells) under these conditions were 15.6 for AN387, 20.1 for JRG2821, 12.7 for JRG2813, and 3.7 for JRG2814.

TABLE 2. V_{max} and K_m values for fumarate uptake in aerobically grown *E. coli*[a]

Strain	K_m (μM fumarate)	V_{max} (μmol/min/g)
AN387	51	69
JRG2821 (*dcuA*::Spc^r)	65	96
JRG2813 (*dcuB*::Kan^r)	62	55
JRG2814 (*dcuA*::Spc^r *dcuB*::Kan^r)	38	58

[a] Uptake of [^{14}C]fumarate in unloaded bacteria was measured, and K_m and V_{max} values were derived from Lineweaver-Burk plots.

substrates across the cytoplasmic membrane was seriously impaired. It would thus appear that the *dcuA* and *dcuB* genes encode the carriers responsible for fumarate-succinate exchange. The properties of the Dcu antiporter(s) match those described previously for the anaerobic C_4-dicarboxylate antiport system with respect to substrate specificity (C_4-dicarboxylates), transport mode (dicarboxylate exchange), and anaerobic function.

Multiple C_4-dicarboxylate transport systems in *E. coli*. This work demonstrates that *dcuA* and *dcuB* encode analogous but independent and mutually complementary anaerobic C_4-dicarboxylate transport systems. The two genes probably specify different C_4-dicarboxylate carriers rather than components of a single system. Moreover, their locations in the *E. coli* linkage map, 94 (*dcuA*) and 93.5 min (*dcuB*), demonstrate that they differ from the *dctA*, *dctB*, and *cbt* genes (78, 16, and 16 min, respectively) encoding the aerobic C_4-dicarboxylate uptake system (1). The combined physiological, biochemical, and genetic evidence unanimously supports the view that *E. coli* expresses distinct and independent aerobic and anaerobic C_4-dicarboxylate transport systems. The residual growth exhibited by the *dcuAB* mutant in glycerol-plus-fumarate medium and residual transport activities further indicate that there may be yet another anaerobic C_4-dicarboxylate transport system(s). The presence of two, and possibly three, Dcu systems may explain why previous attempts to isolate mutants defective in anaerobic dicarboxylate transport by random mutagenesis failed (20a).

Kinetic and functional analyses of anaerobic antiport activity in wild-type *E. coli* gave no sign of the existence of duplicate systems (5, 6). However, studies with single mutants indicate that both systems are very similar with respect to substrate specificity (K_m), V_{max}, and the conditions of synthesis. Even now, it is not clear to what extent *dcuA* and *dcuB* contribute to overall antiport activity with different dicarboxylates under different growth conditions. The similar activities for C_4-dicarboxylate exchange in the wild type and the single *dcuA* and *dcuB* mutants indicate that the loss of one carrier is compensated by increased activity of the alternative carrier. Studies with *dcu-lacZ* fusions might answer questions concerning the different physiological roles of the two systems, and further studies with *dcu* mutants may help to characterize the residual transport mechanisms.

Substrate specificities of the anaerobic dicarboxylate transport systems. The locations of the *dcu* genes immediately downstream and upstream of the anaerobic aspartase and fumarase genes, *aspA-dcuA* and *dcuB-fumB*, suggest that the corresponding carriers might be specific for the corresponding substrates (DcuA for aspartate and fumarate and DcuB for fumarate and malate), but this was not substantiated. Both carriers appeared to have high and comparable affinities for fumarate, succinate, and aspartate, although DcuA had a lower affinity than DcuB for malate both as a substrate and a

competitive inhibitor. It is surprising that *E. coli* contains two such closely related and mutually complementary anaerobic C_4-dicarboxylate transport systems. However, there are increasing numbers of examples in *E. coli* in which enzyme and transport systems are apparently duplicated for unknown reasons.

ACKNOWLEDGMENTS

We thank the European Molecular Biology Organisation for a Short-Term Fellowship (S.S.); the University of Sheffield Research Fund, the Deutsche Forschungsgemeinschaft, and the Fonds der Chemischen Industrie for financial support; and the Science and Engineering Research Council for an Advanced Fellowship (S.C.A.).

We thank Ruth E. Roberts for technical assistance.

REFERENCES

1. **Bachmann, B. J.** 1990. Linkage map of *Escherichia coli* K-12, edition 8. Microbiol. Rev. **54**:130–197.
2. **Bell, P. J., S. C. Andrews, M. N. Sivak, and J. R. Guest.** 1989. Nucleotide sequence of the FNR-regulated fumarase gene (*fumB*) of *Escherichia coli* K-12. J. Bacteriol. **171**:3494–3503.
3. **Bolivar, F., R. L. Rodriguez, P. J. Greene, M. V. Betlach, H. L. Heynecker, H. W. Boyer, J. H. Crosa, and S. Falkow.** 1977. Construction and characterization of new cloning vehicles. II. A multipurpose cloning system. Gene **2**:95–113.
4. **Eisenberg, D., E. Schwarz, M. Komaromy, and R. Wall.** 1984. Analysis of membrane and surface protein sequences with the hydrophobic moment plot. J. Mol. Biol. **179**:125–142.
5. **Engel, P., R. Krämer, and G. Unden.** 1992. Anaerobic fumarate transport in *Escherichia coli* by an *fnr*-dependent dicarboxylate uptake system which is different from the aerobic dicarboxylate uptake system. J. Bacteriol. **174**:5533–5539.
6. **Engel, P., R. Krämer, and G. Unden.** 1994. Transport of C_4-dicarboxylates by anaerobically grown *Escherichia coli*: energetics and mechanism of exchange, uptake and efflux. Eur. J. Biochem. **222**:605–614.
7. **Grosjean, H., and W. Fiers.** 1982. Preferential codon usage in prokaryotic genes: optimal codon-anticodon interaction energy and the selective codon usage in efficiently expressed genes. Gene **18**:199–209.
8. **Guest, J. R., J. S. Miles, R. E. Roberts, and S. A. Woods.** 1985. The fumarase genes of *Escherichia coli*: location of the *fumB* gene and discovery of a new gene (*fumC*). J. Gen. Microbiol. **131**:2971–2984.
9. **Guest, J. R., R. E. Roberts, and R. J. Wilde.** 1984. Cloning of the aspartase gene (*aspA*) of *Escherichia coli*. J. Gen. Microbiol. **130**:1271–1278.
10. **Klein, P., M. Kanehisa, and C. DeLisi.** 1985. The detection and classification of membrane-spanning proteins. Biochim. Biophys. Acta **815**:468–476.
11. **Kohara, Y., K. Akiyama, and K. Isono.** 1987. The physical map of the whole *E. coli* chromosome: application of a new strategy for rapid analysis and sorting of a large genomic library. Cell **50**:495–508.
12. **Kyte, J., and R. F. Doolittle.** 1982. A simple method for displaying the hydropathic character of a protein. J. Mol. Biol. **157**:105–132.
13. **Lo, T. C. Y.** 1977. The molecular mechanism of dicarboxylic acid transport in *Escherichia coli*. J. Supramol. Struct. **7**:463–480.
14. **Maloney, P. C.** 1992. The molecular and cell biology of anion transport by bacteria. Bioessays **14**:757–762.
15. **Marmur, J.** 1964. A procedure for the isolation of deoxyribonucleic acid from microorganisms. Methods Enzymol. **6**:726–739.
16. **Messing, J.** 1983. New M13 vectors for cloning. Methods Enzymol. **101**:20–78.
17. **Miller, J. H.** 1992. A short course in bacterial genetics. Cold Spring Harbor Laboratory, Cold Spring Harbor, N.Y.
18. **Oden, K. L., L. C. DeVeaux, C. R. T. Vibat, J. E. Cronan, Jr., and R. B. Gennis.** 1990. Genomic replacement in *Escherichia coli* K-12 using covalently closed circular plasmid DNA. Gene **96**:29–36.
19. **Prenthi, P., and H. M. Krisch.** 1984. In vitro insertional mutagenesis using a selectable DNA fragment. Gene **29**:303–313.
20. **Sambrook, J., E. F. Fritsch, and T. Maniatis.** 1989. Molecular cloning: a laboratory manual, 2nd ed. Cold Spring Harbor Laboratory, Cold Spring Harbor, N.Y.

20a. **Six, S., G. Unden, and J. R. Guest.** Unpublished data.

21. **Staden, R.** 1984. Graphic methods to determine the function of nucleic acid sequences: a summary of ANALYSEQ options. Nucleic Acids Res. **12**:505–519.
22. **Tabor, S., and C. C. Richardson.** 1987. DNA sequence analysis with a modified bacteriophage T7 DNA polymerase. Proc. Natl. Acad. Sci. USA **84**:4767–4771.
23. **Takagi, J. S., N. Ida, M. Tokushige, H. Sakamoto, and Y. Shimura.** 1985. Cloning and nucleotide sequence of the aspartase gene of *Escherichia coli* W. Nucleic Acids Res. **13**:2063–2074.
24. **Vieira, J., and J. Messing.** 1987. Production of single-stranded plasmid DNA. Methods Enzymol. **153**:3–11.
25. **von Heijne, G.** 1992. Membrane protein structure prediction: hydrophobicity analysis and the positive-inside rule. J. Mol. Biol. **225**:487–494.
26. **Woods, S. A., and J. R. Guest.** 1987. Differential roles of the *Escherichia coli* fumarases and *fnr*-dependent expression of fumarase B and aspartase. FEMS Microbiol. Lett. **48**:219–224.
27. **Woods, S. A., J. S. Miles, R. E. Roberts, and J. R. Guest.** 1986. Structural and functional relationships between fumarase and aspartase. Nucleotide sequences of the fumarase (*fumC*) and aspartase (*aspA*) genes of *Escherichia coli* K12 Biochem. J. **237**: 547–557.